

1 **Influence of open ocean nitrogen supply on the skeletal $\delta^{15}\text{N}$ of modern**
2 **shallow-water scleractinian corals**

3

4 Xingchen T. Wang^{a,*}, Daniel M. Sigman^a, Anne L. Cohen^b, Daniel J. Sinclair^c, Robert M.
5 Sherrell^{c,d}, Kim M. Cobb^e, Dirk V. Erler^f, Jarosław Stolarski^g, Marcelo V. Kitahara^h,
6 Haojia Renⁱ

7 ^a Department of Geosciences, Guyot Hall, Princeton University, Princeton, NJ 08540, USA

8 ^b Department of Marine Geology and Geophysics, Woods Hole Oceanographic Institution, Woods Hole,
9 MA 02540, USA

10 ^c Institute of Marine and Coastal Sciences, Rutgers University, New Brunswick, NJ 08901, USA

11 ^d Department of Earth and Planetary Sciences, Rutgers University, Piscataway, NJ 08854, USA

12 ^e School of Earth and Atmospheric Sciences, Georgia Institute of Technology, Atlanta, GA 30332-0340,
13 USA

14 ^f School of Environment, Science and Engineering, Southern Cross University, Lismore, NSW 2480,
15 Australia

16 ^g Institute of Paleobiology, Polish Academy of Sciences, Twarda 51/55, PL-00-818 Warsaw, Poland

17 ^h Departamento de Ciências do Mar, Universidade Federal de São Paulo, Campus Baixada Santista, Av.
18 Alm. Saldanha da Gama, 89, Ponta da Praia, 11030-400, Santos (SP), Brasil

19 ⁱ Department of Geosciences, National Taiwan University, Taipei 106, Taiwan

20

21 *Corresponding author:

22 Tel: +1 609 937 2536

23 E-mail address: xingchen@princeton.edu

24 **Abstract**

25 The isotopic composition of skeleton-bound organic nitrogen in shallow-water
26 scleractinian corals (hereafter, CS- $\delta^{15}\text{N}$) is an emerging tool for studying the marine
27 nitrogen cycle in the past. The CS- $\delta^{15}\text{N}$ has been shown to reflect the $\delta^{15}\text{N}$ of nitrogen (N)
28 sources to corals, with most applications to date focusing on the anthropogenic/terrestrial
29 N inputs to reef environments. However, many coral reefs receive their primary N
30 sources from the open ocean, and the CS- $\delta^{15}\text{N}$ of these corals may provide information
31 on past changes in the open ocean regional and global N cycle. Using a recently
32 developed persulfate/denitrifier-based method, we measured CS- $\delta^{15}\text{N}$ in modern shallow-
33 water scleractinian corals from 8 sites proximal to the open ocean. At sites with low open
34 ocean surface nitrate concentrations typical of the subtropics and tropics, measured CS-
35 $\delta^{15}\text{N}$ variation on seasonal and annual timescales is most often less than 2‰. In contrast,
36 a broad range in CS- $\delta^{15}\text{N}$ (of ~10‰) is measured across these sites, with a strong
37 correlation between CS- $\delta^{15}\text{N}$ and the $\delta^{15}\text{N}$ of the deep nitrate supply to the surface waters
38 near the reefs. While CS- $\delta^{15}\text{N}$ can be affected by other N sources as well and can vary in
39 response to local reef conditions as well as coral/symbiont physiological changes, this
40 survey indicates that, when considering corals proximal to the open ocean, the $\delta^{15}\text{N}$ of the
41 subsurface nitrate supply to surface waters drives most of the CS- $\delta^{15}\text{N}$ variation across

42 the global ocean. Thus, CS- $\delta^{15}\text{N}$ is a promising proxy for reconstructing the open ocean
43 N cycle in the past.

44 **1. Introduction**

45 Coral skeleton-bound organic matter (CSOM) constitutes 0.01-0.1% of the skeleton
46 material by weight and research is ongoing to understand the synthesis, composition and
47 role of organic matter during the calcification process (Drake et al., 2013; Tambutte et al.,
48 2011). From a paleoceanographic and biogeochemical perspective, the CSOM is directly
49 synthesized by coral at the time of calcification and may provide important information
50 about coral reef environments in the past. For shallow-water scleractinian corals, CSOM
51 has several key virtues as an archive of past conditions. First, CSOM is protected by the
52 carbonate skeleton and may be preserved for tens or hundreds of millions of years
53 (Muscatine et al., 2005). Second, shallow-water scleractinian corals are widely
54 distributed in the low latitude ocean, and fossil coral samples are found throughout the
55 Mesozoic and Cenozoic Eras (i.e. back to ~240 Ma). Third, shallow-water scleractinian
56 corals have high linear extension rates (e.g., 2 cm/year) and produce annual growth bands.
57 Appropriate techniques would allow for the generation of high-resolution records on
58 individual coral cores.

59

60 Due to the difficulty associated with analyzing this dilute form of organic matter, only a
61 handful of measurements have been made on CSOM: total organic carbon and amino
62 acid composition (Ingalls et al., 2003), carbon isotopes (Muscatine et al., 2005) and
63 nitrogen isotopes (Erler et al., 2015; Hoegh-Guldberg et al., 2004; Marion et al., 2005;
64 Muscatine et al., 2005; Wang et al., 2015). Among these measurements, a recent
65 analytical advance in nitrogen isotopic analysis of CSOM (hereafter: CS- $\delta^{15}\text{N}$) requires
66 only 5-10 mg of carbonate material per measurement and yields a precision of 0.2‰
67 (Wang et al., 2015). Thus, this technique allows for the generation of seasonal or even
68 monthly CS- $\delta^{15}\text{N}$ records on single coral cores that are comparable to other records made
69 on the inorganic carbonate of corals (e.g., $\delta^{18}\text{O}$, Metal/Ca ratio) (Erler et al., 2016).

70

71 CS- $\delta^{15}\text{N}$ in shallow-water scleractinian corals has been shown to reflect the $\delta^{15}\text{N}$ of N
72 sources to corals. Most studies to date have focused on anthropogenic/terrestrial N input
73 into the reefs (Erler et al., 2015; Hoegh-Guldberg et al., 2004; Jupiter et al., 2008; Marion
74 et al., 2005). However, the water over many reefs exchanges freely with open ocean
75 surface waters, and the CS- $\delta^{15}\text{N}$ in corals from these reefs is expected to reflect the $\delta^{15}\text{N}$
76 of open ocean N supply, an expectation that is supported by some recent data (Yamazaki

77 et al., 2011). If this applies generally, then it would expand the range of potential
78 applications of CS- $\delta^{15}\text{N}$ to studies of past changes in the open ocean N cycle, on
79 timescales ranging from recent centuries to the distant geological past. In this study,
80 using corals from 8 globally distributed sites, we test the hypothesis that CS- $\delta^{15}\text{N}$ of
81 corals proximal to the open ocean is controlled by the $\delta^{15}\text{N}$ of oceanic nitrate supplied to
82 the euphotic zone adjacent to the reefs.

83

84 **2. Materials and methods**

85 **2.1 Corals**

86 The coral samples used in this study are from the following sites (**Figure 1; Table 1**):
87 Bermuda in the North Atlantic, the Brazil margin in the South Atlantic, the Oman margin
88 in the Indian Ocean, the northern Great Barrier Reef (GBR), New Caledonia, the
89 Dongsha atoll and Green Island in the western Pacific, and Kiritimati Island in the central
90 equatorial Pacific (CEP). The sampling was proximal to the open ocean, and there is no
91 distinctively large terrestrial input into any of these sites, increasing the likelihood that
92 they directly reflect the $\delta^{15}\text{N}$ of oceanic N sources. We have measured CS- $\delta^{15}\text{N}$ from
93 such locations as the inshore Great Barrier Reef (Erlor et al., 2015) and lagoon patch
94 reefs nearby the islands of Bermuda (Wang et al., 2015), but these are not included in our

95 analysis. From the Bermuda pedestal, we use only the offshore corals that we have
96 measured (Wang et al., 2015). At each site, coral heads from one or multiple colonies
97 were collected from living corals by scuba divers. Collection information for each site is
98 given in **Table 1** and **supplementary Figure 1**. The Pacific and Indian Ocean coral
99 samples in this study are *Porites. sp.*, except for the New Caledonia coral (*Isopora*
100 *palifera*); while the Atlantic coral samples include three species: *Diploria*
101 *labyrinthiformis* for Bermuda; and *Mussismilia hispida* and *Madracis decactis* for Brazil
102 Margin. Despite the species differences, all the corals used in this study are symbiotic (i.e.
103 have zooxanthellae).

104

105 In the lab, a slab was cut from each coral head for *Porites* and *Diploria*. The *Porites* and
106 *Diploria* slabs were rinsed with deionized water, dried, and then scanned by computed
107 axial tomography (CAT) to determine the maximum growth axis. Age models of the
108 *Porites* and *Diploria* slabs were determined by counting annual growth bands in CAT
109 scan images or by correlating with Sr/Ca records in the same core. Along the maximum
110 growth axis, powder samples were drilled out from each slab/piece at annual/seasonal
111 resolution. For coral species other than *Porites* and *Diploria*, no age model was generated.
112 Tissue from these corals was removed with a jet of deionized water. Then skeleton pieces

113 were cut from the coral skeleton with a rotary tool and diamond-coated cutting wheel.
114 The skeleton pieces were rinsed with deionized water, dried and crushed into fine powder
115 with agate mortar and pestle. These pieces were estimated to represent several years'
116 growth. **Table 1** describes the samples accumulated into the average CS- $\delta^{15}\text{N}$ reported
117 for each site.

118

119 **2.2 CS- $\delta^{15}\text{N}$ measurements**

120 The coral carbonate powders were analyzed for CS- $\delta^{15}\text{N}$ following the protocol in (Wang
121 et al., 2015). First, in an oxidative cleaning step, 10 mL sodium hypochlorite (10-15%
122 available chlorine) is added to 5-10 mg of coral powder in 15 mL centrifuge tubes. These
123 centrifuge tubes are placed on an orbital shaker for 24 hours. The oxidative cleaning step
124 has been demonstrated to be important for the removal of contaminant organic matter
125 (Hendy et al., 2012; Ingalls et al., 2003; Ramos-Silva et al., 2013) and thus the analysis of
126 CS- $\delta^{15}\text{N}$ (Erler et al., 2016; Wang et al., 2015). The cleaning reagent is decanted, and the
127 sample is rinsed 3 times with deionized water by centrifugation and decanting and then
128 dried at 60°C. Once dry, the sample is weighed into a 4 mL borosilicate glass vial
129 (precombusted for 5 hours at 500°C) and dissolved by reaction with 4 N HCl. After
130 dissolution, an aliquot of 1 mL freshly combined persulfate oxidizing reagent (1 g

131 recrystallized low-N potassium persulfate and 2 g ACS grade NaOH in 100 mL deionized
132 water) is added, and the sample is autoclaved for 1.5 hour to completely oxidize to nitrate
133 the organic nitrogen released during decalcification. After oxidation, the sample is
134 centrifuged; the clear supernatant is transferred to another precombusted 4 mL
135 borosilicate glass vial and the pH of the supernatant is adjusted to near 7 with HCl and
136 NaOH. The nitrate concentration of the sample solution is analyzed by
137 chemiluminescence (Braman and Hendrix, 1989), mostly to determine aliquot volumes
138 for $\delta^{15}\text{N}$ measurement. The $\delta^{15}\text{N}$ of the nitrate is measured by conversion to N_2O with the
139 “denitrifier method” (Sigman et al., 2001) followed by extraction, purification, and
140 isotopic analysis of the N_2O product (Casciotti et al., 2002). Amino acid reference
141 materials USGS 40 and 41 are used in each batch of analyses to correct for the reagent
142 and operational blanks, which is typically less than 2% of the total N content in an
143 oxidized sample. An in-house coral standard (CBS-1) provides a metric for
144 reproducibility both within an analysis batch and across batches. The analytical precision
145 (1sd) of our protocol is 0.2‰ (Wang et al., 2015). For each coral core, an average CS-
146 $\delta^{15}\text{N}$ (\pm 1sd) is calculated from the time-series data. For each site, an average CS- $\delta^{15}\text{N}$ (\pm
147 1sd) is calculated from all coral cores (**Table 1**).

148

149 **3. Results**

150 At each site, CS- $\delta^{15}\text{N}$ shows relatively weak temporal and spatial variability (1sd <1‰,
151 **Table 1**), with a range of <3‰ in any single core (**Table 1**). The difference in CS- $\delta^{15}\text{N}$
152 between species is only 1.1‰ at Brazil margin, consistent with a previous study off-shore
153 of Heron Island in the Great Barrier Reef suggesting a difference between two coral
154 species of 1.1‰ (Erlor et al., 2015). In contrast, among the 8 sites, we observe a broad
155 range of ~10‰ in CS- $\delta^{15}\text{N}$, with the highest values on Kiritimati Island ($13.4 \pm 0.5\text{‰}$)
156 and the lowest values on Bermuda ($4.1 \pm 0.5\text{‰}$) and Green Island ($4.2 \pm 0.6\text{‰}$). The
157 Brazil Margin corals and Oman margin corals show a relatively high CS- $\delta^{15}\text{N}$ of $8.8 \pm$
158 0.8‰ and $10.1 \pm 0.2\text{‰}$, respectively. The Northern Great Barrier Reef, New Caledonia
159 and Dongsha atoll corals show a similar CS- $\delta^{15}\text{N}$ of $6.2 \pm 0.6\text{‰}$, $6.2 \pm 0.3\text{‰}$, and $5.9 \pm$
160 0.5‰ , respectively.

161

162 **4. Interpretation and discussion**

163 Even without considering global warming and ocean acidification, anthropogenic impacts
164 threaten many coral reefs (Hughes et al., 2003). One major anthropogenic factor is the
165 increasing nutrient transport into inshore reefs (e.g., inshore South Great Barrier Reef;
166 (Brodie et al., 2011)). For this reason, a number of coral $\delta^{15}\text{N}$ studies has focused on

167 tracking anthropogenic/terrestrial N inputs to coral reefs (Baker et al., 2010; Erler et al.,
168 2015; Jupiter et al., 2008; Marion et al., 2005; Yamazaki et al., 2011). However, many
169 coral reefs are far from terrestrial N sources and must rely on N supplied from the open
170 ocean. It is thus expected that the CS- $\delta^{15}\text{N}$ of these corals should reflect the $\delta^{15}\text{N}$ of
171 oceanic N sources. Below, we compare our CS- $\delta^{15}\text{N}$ results with the $\delta^{15}\text{N}$ of oceanic N
172 supplied to the reef from which each coral derives.

173

174 In laboratory experiments, symbiotic corals have been demonstrated to access N from a
175 range of sources, including particulate organic matter and plankton ingestion
176 (Houlbrèque and Ferrier-Pagès, 2009) as well as ammonium and nitrate assimilation
177 (Badgley et al., 2006; Grover et al., 2002; Tanaka et al., 2006). However, in the real
178 ocean, symbiotic corals in a given region likely rely on a more limited set of N forms,
179 depending on availability. For example, in oligotrophic waters such as Bermuda, the
180 surface ocean concentrations of ammonium and nitrate are less than 20 nM (Fawcett et al.,
181 2014; Lomas et al., 2013), well below the assimilation thresholds found in lab
182 experiments (Badgley et al., 2006; Tanaka et al., 2006). In such systems, the ultimate N
183 source is dominantly the nitrate from wintertime deep mixing or upwelling (Altabet, 1988;

184 Knapp et al., 2005), while the N available to the corals is mostly in organic forms that
185 were produced from this nitrate by phytoplankton assimilation, followed by upper ocean
186 N cycling and the phytoplankton assimilation of ammonium. In contrast, in upwelling
187 systems such as the central and eastern equatorial Pacific, surface nitrate concentrations
188 can be high. As a result, symbiotic corals in such systems might use nitrate from the open
189 ocean or organic N produced over the reef or imported from the open ocean. Accordingly,
190 we first divide the 8 coral sites in this study into two categories based on the whether the
191 adjacent surface ocean nitrate is fully consumed. Among our 8 coral sites, only the CEP
192 coral site (Kiritimati Island) is from an ocean region where the mixed layer nitrate is
193 frequently at micromolar levels. Even at the Oman site, which hosts seasonal offshore
194 upwelling associated with the Indian summer monsoons, there is rarely significant unused
195 nitrate in the waters over the reef or immediately offshore (World Ocean Atlas 2013).
196 Thus, we group it with the corals from reefs with low surface nitrate concentrations; this
197 decision is discussed further in Section 4.2.

198

199 **4.1 Corals from low nutrient ocean regions**

200 In ocean regions where the annual mean mixed layer concentration of inorganic N is less
201 than roughly 0.5 μM , the assimilation of inorganic N by corals is probably too slow for
202 them to be significant, especially when food is available (Grover et al., 2002). Only in
203 experiments where corals are starved is there evidence for significant nitrate/ammonium
204 uptake, and then mostly at concentrations above $\sim 2 \mu\text{M}$ (Badgley et al., 2006; Tanaka et
205 al., 2006). If this view of inorganic N uptake is correct, corals in most tropical ocean
206 regions must dominantly rely on organic matter as their N source. The $\delta^{15}\text{N}$ of euphotic
207 zone biomass in these regions is expected to covary with the $\delta^{15}\text{N}$ of nitrate below the
208 euphotic zone, which reflects the $\delta^{15}\text{N}$ of the nitrate supply to the euphotic zone, and the
209 available data support this expectation (Fawcett et al., 2011; Graham et al., 2010; Lorrain
210 et al., 2015; Montoya et al., 2002; Ren et al., 2012). Thus, for all our coral sites except
211 the CEP site, we compare CS- $\delta^{15}\text{N}$ to the $\delta^{15}\text{N}$ of subsurface nitrate (**Figure 2**).

212

213 It is more challenging to address which specific fractions of particulate organic matter in
214 the water column are accessed by corals. At Bermuda, the $\delta^{15}\text{N}$ of bulk suspended
215 particulate organic nitrogen (PON) in the surface ocean is $<0\text{‰}$, as is the $\delta^{15}\text{N}$ of the
216 dominant prokaryotic phytoplankton (Fawcett et al., 2011). However, larger biological

217 particles such as eukaryotic phytoplankton and zooplankton are higher in $\delta^{15}\text{N}$ (Fawcett
218 et al., 2011; Montoya et al., 2002), and many investigators would argue that these are
219 more important prey items for corals (Houlbrèque and Ferrier-Pagès, 2009). At Bermuda
220 near Hog Reef (a northern fringing reef), the average $\delta^{15}\text{N}$ of net tow-collected plankton
221 larger than 35 μm is 3.5-4‰ (Wang et al., 2015), similar to the CS- $\delta^{15}\text{N}$ at this location
222 (**Table 1**). A study of two coral species suggested that CS- $\delta^{15}\text{N}$ was indistinguishable
223 from the coral tissue $\delta^{15}\text{N}$ in one species and 1-1.5‰ higher than the coral tissue $\delta^{15}\text{N}$ in
224 the other (Erler et al., 2015). The CS- $\delta^{15}\text{N}$ /tissue $\delta^{15}\text{N}$ offset and any variation among
225 species are of interest. In any case, the data from Hog Reef imply that coral tissue $\delta^{15}\text{N}$ is
226 similar to (not clearly higher than) the $\delta^{15}\text{N}$ of their food source. This fits into a broader
227 interpretation of coral $\delta^{15}\text{N}$ data (Wang et al., 2015), in which corals recycle their
228 metabolic ammonium to their symbionts (Falkowski et al., 1993; Kopp et al., 2013;
229 Tanaka et al., 2006), reducing their elevation in $\delta^{15}\text{N}$ relative to their food source below
230 the ~3.5‰ typical of heterotrophs (Minagawa and Wada, 1984).

231

232 The shallow-water scleractinian corals used in this study are from regions that cover a
233 range of subsurface nitrate $\delta^{15}\text{N}$, due to the hydrography and biogeochemistry of each

234 ocean region. The Sargasso Sea and South China Sea coral sites are characterized by low
235 subsurface nitrate $\delta^{15}\text{N}$, primarily due to N fixation (Kao et al., 2012; Knapp et al., 2008).
236 The Arabian Sea coral site has a high subsurface nitrate $\delta^{15}\text{N}$, apparently caused by
237 mixing with the underlying water column denitrification zones, which preferentially
238 removes ^{14}N -nitrate relative to ^{15}N -nitrate and leaves the residual nitrate enriched in ^{15}N
239 (Brandes et al., 1998). The South Atlantic coral site is characterized by a subsurface
240 nitrate $\delta^{15}\text{N}$ 1-2‰ higher than deep ocean nitrate $\delta^{15}\text{N}$ (Frame, 2011; Smart et al., 2015),
241 which is attributed to incomplete nitrate consumption in the Southern Ocean and
242 northward transport of Subantarctic Mode Water and Antarctica Intermediate Water
243 (Smart et al., 2015). The northern Great Barrier Reef and New Caledonia appears to have
244 a subsurface nitrate $\delta^{15}\text{N}$ of 6.1‰, slightly higher than the deep ocean nitrate $\delta^{15}\text{N}$ in the
245 same region (Yoshikawa et al., 2015).

246

247 **4.2 Corals from nitrate-rich upwelling ocean regions**

248 In the eastern and central equatorial Pacific, easterly trade winds drive upwelling of cool
249 and nutrient-rich waters. Phytoplankton assimilates only a portion of the upwelled nitrate
250 at the equator, with the remaining nitrate being drawn down as it is advected off axis

251 **(Figure 3A)**. Due to isotope fractionation during nitrate assimilation, the decline in
252 nitrate concentration from the subsurface into the surface and northward and southward
253 from the equator is accompanied by a rise in the $\delta^{15}\text{N}$ of nitrate, following the path of the
254 upwelled water parcel (Altabet and Francois, 1994; Rafter et al., 2012). In the CEP, the
255 surface water is dominantly sourced from the underlying Equatorial Under Current
256 (EUC), which has a nitrate concentration of $12.4 \pm 2.5 \mu\text{M}$ and a nitrate $\delta^{15}\text{N}$ of $7.2 \pm 0.3\text{‰}$
257 (Rafter and Sigman, 2016). Most data from the CEP indicate the consumption of nitrate
258 without resupply subsequent to upwelling into the euphotic zone, consistent with the
259 Rayleigh model, and the isotope effect of nitrate assimilation estimated from the
260 Rayleigh model substrate equation is $6.0 \pm 0.4\text{‰}$ (Rafter and Sigman, 2016).

261

262 In contrast to corals from low nutrient regions, there are three potential oceanic N sources
263 for the CEP corals, and the Rayleigh model can be used to estimate the $\delta^{15}\text{N}$ of these N
264 sources given the isotopic parameters described above and the climatological annual
265 mean mixed layer nitrate concentrations **(Figure 3)**: (1) surface water nitrate (from the
266 substrate equation of the Rayleigh model); (2) euphotic zone PON accumulated since the
267 time of upwelling (from the integrated product of the Rayleigh model); and PON
268 generated over the reefs from mixed layer nitrate imported from the open ocean (from the

269 instantaneous product of the Rayleigh model). Due to the limited data on these reefs, it is
270 challenging to identify the dominant N sources to the corals. Among the three N sources
271 described above, we expect that the Kiritimati coral obtains its N primarily by feeding on
272 the PON generated on the reef as the nitrate is consumed. Several lines of evidence
273 support this hypothesis. The CS- $\delta^{15}\text{N}$ data from Kiritimati Island coral ($13.4 \pm 0.5\text{‰}$) are
274 closest to the $\delta^{15}\text{N}$ of PON expected from the instantaneous product of the Rayleigh
275 model ($\sim 11\text{‰}$, **Figure 3B**), given the open ocean euphotic zone nitrate concentrations
276 adjacent to the reefs as well as the available Kiritimati reef nitrate/nitrite concentration
277 data (**Figure 3B**) (Dinsdale et al., 2008; Rafter and Sigman, 2016). In addition, Kiritimati
278 Island sits at 2°N , outside of the core upwelling zone at the equator. It is unlikely that
279 PON produced since the time of upwelling (as would be approximated by the integrated
280 product of the Rayleigh model) can travel so far north without being exported to depth.
281 Further, given prior data on the relationship between co-occurring PON $\delta^{15}\text{N}$ and CS-
282 $\delta^{15}\text{N}$ (Wang et al., 2015; Erler et al., 2015), feeding on PON accumulated in the open
283 ocean euphotic zone, as simulated by the integrated product of the Rayleigh model,
284 would be expected to yield a CS- $\delta^{15}\text{N}$ $\sim 9\text{‰}$ lower than we measured.
285

286 Corals are capable of assimilating nitrate (Badgley et al., 2006; Tanaka et al., 2006), and
287 the process is often elicited in laboratory studies by starving corals, that is, foregoing
288 purposeful feeding. There are almost certainly oceanic conditions under which corals
289 make use of nitrate assimilation. However, we consider it unlikely that nitrate
290 assimilation is the primary N source for corals at Kiritimati. Nitrate taken up by the coral
291 symbiotic system is assimilated into biomass by the zooxanthellae, and yet the
292 zooxanthellae cytoplasm is separated from ambient water by 3 membranes or more. This
293 provides a basic mechanistic reason that corals would undertake minimal nitrate
294 assimilation under low nitrate concentrations and/or when PON availability is high.
295 Moreover, because nitrate must efflux back into the environment for nitrate assimilation
296 to drive significant isotope fractionation (Karsh et al., 2014; Needoba et al., 2004), the
297 multiple cell boundaries lead to the expectation that isotope fractionation during nitrate
298 assimilation will be low, especially at low nitrate concentrations. Indeed, this effect has
299 been observed in culture experiments, such that at a seawater nitrate concentration
300 relevant to the Kiritimati Island (i.e. 2-3 μM), the isotope effect of nitrate assimilation is
301 only $\sim 2\text{‰}$ (Devlin, 2015). Complete reliance on coral nitrate assimilation could be
302 argued to be inconsistent with the observation that the nitrate $\delta^{15}\text{N}$ is 3-4 ‰ higher than
303 the CS- $\delta^{15}\text{N}$ (**Figure 3B**). Nevertheless, given the uncertainties in this comparison, we

304 cannot rule out the possibility of dominant or partial reliance on nitrate assimilation. The
305 combined occurrence of nitrate assimilation and feeding by Kiritimati corals is clearly
306 possible on the basis of the isotopic comparison, as CS- $\delta^{15}\text{N}$ falls in between the $\delta^{15}\text{N}$ of
307 these two N sources (**Figure 3B**).

308

309 Because the subsurface nitrate supply is only partially consumed in CEP surface waters,
310 the $\delta^{15}\text{N}$ of the subsurface nitrate near Kiritimati is not an appropriate measure of the
311 $\delta^{15}\text{N}$ of the N available to the coral. Accordingly, in **Figure 2**, the parameter applied to
312 the x-axis for the Kiritimati coral is different from that of the other 7 sites. Because of the
313 ambiguity associated with feeding versus nitrate assimilation, we show symbols for both
314 the average $\delta^{15}\text{N}$ of mixed layer nitrate at a set of stations (155 °W, 0-1 °N) adjacent to
315 Kiritimati and the calculated $\delta^{15}\text{N}$ of instantaneous PON as the x-axis parameter in
316 **Figure 2**. To indicate this difference in x-axis parameter in **Figure 2**, the Kiritimati coral
317 is indicated with two open (rather than filled) symbols.

318

319 It should be asked whether the above interpretation is applicable to reefs adjacent to
320 coastal upwelling such as the Oman margin coral. The open ocean surface waters off the
321 Oman margin are strongly influenced by the Indian Monsoon system. During the summer

322 (late June to early October), the southwestern monsoon induces Ekman upwelling, with
323 non-zero nitrate during the summer upwelling period (World Ocean Atlas 2013). During
324 the rest of the year (middle October to middle June), nitrate drops to oligotrophic open
325 ocean levels (**Figure 4**). If nitrate assimilation in the waters overlying the Oman margin
326 coral is an important source of PON to the coral, based on the instantaneous product
327 equation of the Rayleigh model, a summertime decrease of $\sim 2\text{‰}$ would be expected in
328 the coral $\delta^{15}\text{N}$. In contrast, a seasonally resolved Oman margin CS- $\delta^{15}\text{N}$ record suggests
329 very little ($\sim 0.5\text{‰}$) variation, with slightly higher CS- $\delta^{15}\text{N}$ observed in the summer
330 (**Figure 4**). Moreover, as described below, the CS- $\delta^{15}\text{N}$ of the Oman coral is consistent
331 with the relationship observed among the corals from oligotrophic sites. These
332 observations suggest that open ocean-produced PON is the dominant N source to the
333 Oman margin reefs. The difference from the CEP coral is consistent with the high
334 productivity in the Oman upwelling and complete consumption of nitrate prior to
335 transport of the open ocean waters onto the Oman margin. While we cannot be confident
336 that the same situation will apply across all coastal upwelling systems, this would appear
337 likely: coastal upwelling systems typically involve consumption of the upwelled nutrients
338 near the site of upwelling, and any lateral transport of residual nutrients is most often
339 offshore rather than onshore.

340

341 **4.3 Global comparison of CS- $\delta^{15}\text{N}$ to the subsurface nitrate $\delta^{15}\text{N}$**

342 Comparing CS- $\delta^{15}\text{N}$ to the the subsurface nitrate $\delta^{15}\text{N}$, we observe a strong linear
343 correlation ($R^2 = 0.82$, **Figure 2**). The average difference between CS- $\delta^{15}\text{N}$ and the
344 subsurface nitrate $\delta^{15}\text{N}$ (excluding Kiritimati Island) is $0.8 \pm 0.8\%$. These values indicate
345 that CS- $\delta^{15}\text{N}$ is only slightly higher than the $\delta^{15}\text{N}$ of subsurface nitrate supplied to the
346 reefs. This observation is consistent with previous findings that (1) corals feed on a
347 PON/plankton pool that resembles the $\delta^{15}\text{N}$ of the nitrate supplied to and consumed in the
348 euphotic zone, and (2) symbiotic corals do not exhibit the $\sim 3\%$ trophic $\delta^{15}\text{N}$ elevation
349 because of minimal loss of low- $\delta^{15}\text{N}$ ammonium to the oligotrophic waters (Reynaud et
350 al., 2009; Wang et al., 2015). From a paleoceanographic perspective, the strong
351 correlation indicates that, for corals that are proximal to the open water, the subsurface
352 nitrate $\delta^{15}\text{N}$ is the dominant control on CS- $\delta^{15}\text{N}$.

353

354 **4.4 Implications for paleoceanography**

355 The strong correlation between the CS- $\delta^{15}\text{N}$ and the $\delta^{15}\text{N}$ of subsurface nitrate suggests
356 that CS- $\delta^{15}\text{N}$ will be a powerful tool for studying the past marine N cycle. Ocean

357 sediments are the primary existing archives for reconstructing marine N cycling in the
358 past. Bulk sedimentary $\delta^{15}\text{N}$, microfossil-bound $\delta^{15}\text{N}$ and compound-specific $\delta^{15}\text{N}$ from
359 sediments have all contributed to our understanding of the past marine N cycle. Relative
360 to these sediment-based archives, shallow-water scleractinian corals have the potential to
361 record orders of magnitude higher temporal resolution, due to substantial skeletal growth
362 rates and the lack of a smoothing process akin to the bioturbation of sediments. Direct
363 absolute age dating as well as annual band counting will improve the dating of N cycle
364 changes and allow for N cycle-focused studies of short time scale phenomena such as El
365 Niño-Southern Oscillation.

366

367 Deep-sea corals (both proteinaceous corals and scleractinian corals) have also been
368 explored as an archive for studying the past marine N cycle (Sherwood et al., 2014;
369 Wang et al., 2014). In comparison to proteinaceous corals, scleractinian corals have the
370 advantage that the carbonate skeleton can protect the CSOM for hundreds of millions of
371 years, and more broadly, diagenesis is less of a concern. In comparison to the deep-sea
372 corals, shallow-water scleractinian corals have the advantages that the samples are widely
373 accessible and that the potential time resolution of the records is much higher.

374

375 One possible complication of using CS- $\delta^{15}\text{N}$ as a N cycle proxy is the previously
376 suggested effect of feeding rate on the coral/symbiont N cycle and its consequences for
377 the $\delta^{15}\text{N}$ of the coral system (Wang et al., 2015). It was observed that in highly
378 productive inshore waters of Bermuda pedestal, the CS- $\delta^{15}\text{N}$ is $\sim 3\text{‰}$ higher than that of
379 the Bermuda outer reef corals discussed here, with $\sim 2\text{‰}$ of this difference deriving from
380 a change in CS- $\delta^{15}\text{N}$ relative to the $\delta^{15}\text{N}$ of its N source. This finding was explained as
381 the result of ammonium leakage out of the coral symbiotic system when corals increase
382 their feeding rates in the highly productive inshore waters.

383

384 For corals that are proximal to the oligotrophic tropical and subtropical ocean, the
385 productivity effect is probably minor (e.g., in the case of offshore corals at Bermuda).
386 Indeed, the strength of correlation between CS- $\delta^{15}\text{N}$ and the $\delta^{15}\text{N}$ of nitrate consumed
387 across the corals studied to date (**Figure 2**) suggests that variation in “baseline $\delta^{15}\text{N}$ ”
388 overshadows other processes in setting the CS- $\delta^{15}\text{N}$ of a given coral. Further modern
389 studies that benefit from robust information on environmental variables at a study site
390 (e.g., water column productivity, nutrient concentrations) may allow the individual

391 effects on CS- $\delta^{15}\text{N}$ of source $\delta^{15}\text{N}$ and productivity to be diagnosed more completely. In
392 coral cores, a correlation between CS- $\delta^{15}\text{N}$ and coral extension rate is observed among
393 the Bermuda corals (Logan et al., 1994; Wang et al., 2015), which might allow for
394 attribution of certain downcore CS- $\delta^{15}\text{N}$ changes to the tightness of the coral's internal N
395 recycling as opposed to baseline $\delta^{15}\text{N}$. More generally, parallel measurements of CS- $\delta^{15}\text{N}$
396 and other proxies (e.g., coral extension rate, $\delta^{13}\text{C}$, $\delta^{11}\text{B}$) could yield complementary
397 information that will compensate for the uncertainties of individual proxies.

398

399 In the near term, we consider it simpler to interpret CS- $\delta^{15}\text{N}$ from coral sites near reef
400 margins in nutrient-poor ocean regions, where there is not the potential for variable, large
401 scale inputs of oceanic nitrate onto the reef and where feeding changes are less likely to
402 drive coral host/symbiont effects on CS- $\delta^{15}\text{N}$. In the same sense, CS- $\delta^{15}\text{N}$ is in the
403 greatest need of further ground-truthing in nutrient-rich oceanic regions and/or in inshore
404 reef systems.

405

406

407 **Acknowledgements**

408 This work was supported by the NSF Grants OCE-1060947 and OCE-1536368 to D.M.S.
409 and OCE-1537338 to A.L.C, the MacArthur Foundation (D.M.S.), the Grand Challenges
410 Program at Princeton University (D.M.S.), the Schlanger Fellowship Program of the
411 Consortium for Ocean Leadership (X.T.W.), the Charlotte Elizabeth Procter Fellowship
412 of the Graduate School at Princeton University (X.T.W.) and a Graduate Student
413 Research Grant from the Geological Society of America (X.T.W.). We thank A. Alpert
414 and B. Jonsson for helpful discussions and two anonymous reviewers for insightful
415 comments.

416

417

418

419

420

421

422

423 **References**

- 424 Altabet, M.A., 1988. Variations in nitrogen isotopic composition between sinking and
425 suspended particles: implications for nitrogen cycling and particle transformation in
426 the open ocean. *Deep Sea Res. A* 35, 535–554. doi:10.1016/0198-0149(88)90130-6
- 427 Altabet, M.A., Francois, R., 1994. Sedimentary Nitrogen Isotopic Ratio as a Recorder for
428 Surface Ocean Nitrate Utilization. *Global Biogeochem Cycles* 8, 103–116.
429 doi:10.1029/93GB03396
- 430 Badgley, B.D., Lipschultz, F., Sebens, K.P., 2006. Nitrate uptake by the reef coral
431 *Diploria strigosa*: effects of concentration, water flow, and irradiance. *Mar. Biol.* 149,
432 327–338. doi:10.1007/s00227-005-0180-5
- 433 Baker, D.M., Jordan-Dahlgren, E., Angel Maldonado, M., Harvell, C.D., 2010. Sea fan
434 corals provide a stable isotope baseline for assessing sewage pollution in the Mexican
435 Caribbean. *Limnol. Oceanogr.* 55, 2139–2149. doi:10.4319/lo.2010.55.5.2139
- 436 Braman, R.S., Hendrix, S.A., 1989. Nanogram Nitrite and Nitrate Determination in
437 Environmental and Biological-Materials by Vanadium(III) Reduction with Chemi-
438 Luminescence Detection. *Anal. Chem.* 61, 2715–2718. doi:10.1021/ac00199a007
- 439 Brandes, J.A., Devol, A.H., Yoshinari, T., Jayakumar, D.A., Naqvi, S., 1998. Isotopic
440 composition of nitrate in the central Arabian Sea and eastern tropical North Pacific:
441 A tracer for mixing and nitrogen cycles. *Limnol. Oceanogr.* 43, 1680–1689.
442 doi:10.4319/lo.1998.43.7.1680
- 443 Brodie, J.E., Devlin, M., Haynes, D., Waterhouse, J., 2011. Assessment of the
444 eutrophication status of the Great Barrier Reef lagoon (Australia). *Biogeochemistry*
445 106, 281–302. doi:10.1007/s10533-010-9542-2
- 446 Casciotti, K.L., Sigman, D.M., Hastings, M.G., Böhlke, J.K., Hilkert, A., 2002.
447 Measurement of the oxygen isotopic composition of nitrate in seawater and
448 freshwater using the denitrifier method. *Anal. Chem.* 74, 4905–4912.
449 doi:10.1021/ac020113w
- 450 Devlin, Q., 2015. Nutrient Dynamics in the Coral-Algal Symbiosis: Developing Insight
451 from Biogeochemical Techniques.
452 doi:http://scholarlyrepository.miami.edu/oa_dissertations/1514
- 453 Dinsdale, E.A., Pantos, O., Smriga, S., Edwards, R.A., Angly, F., Wegley, L., Hatay, M.,
454 Hall, D., Brown, E., Haynes, M., Krause, L., Sala, E., Sandin, S.A., Thurber, R.V.,
455 Willis, B.L., Azam, F., Knowlton, N., Rohwer, F., 2008. Microbial Ecology of Four
456 Coral Atolls in the Northern Line Islands. *PLoS ONE* 3, e1584.
457 doi:10.1371/journal.pone.0001584

458 Drake, J.L., Mass, T., Haramaty, L., Zelzion, E., Bhattacharya, D., Falkowski, P.G., 2013.
459 Proteomic analysis of skeletal organic matrix from the stony coral *Stylophora*
460 *pistillata*. *Proc. Natl. Acad. Sci. U.S.A.* 110, 3788–3793.
461 doi:10.1073/pnas.1301419110

462 Erler, D.V., Wang, X.T., Sigman, D.M., Scheffers, S.R., Martinez-Garcia, A., Haug,
463 G.H., 2016. Nitrogen isotopic composition of organic matter from a 168 year-old
464 coral skeleton: Implications for coastal nutrient cycling in the Great Barrier Reef
465 Lagoon. *Earth Planet. Sci. Lett.* 434, 161–170. doi:10.1016/j.epsl.2015.11.023

466 Erler, D.V., Wang, X.T., Sigman, D.M., Scheffers, S.R., Shepherd, B.O., 2015. Controls
467 on the nitrogen isotopic composition of shallow water corals across a tropical reef
468 flat transect. *Coral Reefs* 34, 329–338. doi:10.1007/s00338-014-1215-5

469 Falkowski, P.G., Dubinsky, Z., Muscatine, L., McCloskey, L., 1993. Population Control
470 in Symbiotic Corals. *BioScience* 43, 606–611. doi:10.2307/1312147

471 Fawcett, S.E., Lomas, M.W., Casey, J.R., Ward, B.B., Sigman, D.M., 2011. Assimilation
472 of upwelled nitrate by small eukaryotes in the Sargasso Sea. *Nat Geosci* 4, 717–722.
473 doi:10.1038/ngeo1265

474 Fawcett, S.E., Lomas, M.W., Ward, B.B., Sigman, D.M., 2014. The counterintuitive
475 effect of summer-to-fall mixed layer deepening on eukaryotic new production in the
476 Sargasso Sea. *Global Biogeochem Cycles* 28, 86–102. doi:10.1002/2013GB004579

477 Frame, C., 2011. *The Biogeochemistry of Marine Nitrous Oxide*.
478 doi:http://hdl.handle.net/1721.1/68887

479 Graham, B.S., Koch, P.L., Newsome, S.D., McMahon, K.W., Aurioles, D., 2010. Using
480 Isoscapes to Trace the Movements and Foraging Behavior of Top Predators in
481 Oceanic Ecosystems, in: West, J.B., Bowen, G.J., Dawson, T.E., Tu, K.P. (Eds.),
482 *Isoscapes*. Springer Netherlands, Dordrecht, pp. 299–318. doi:10.1007/978-90-481-
483 3354-3_14

484 Grover, R., Maguer, J.-F., Reynaud-Vaganay, S., Ferrier-Pagès, C., 2002. Uptake of
485 Ammonium by the Scleractinian Coral *Stylophora pistillata*: Effect of Feeding Light,
486 and Ammonium Concentrations. *Limnol. Oceanogr.* 47, 782–790.
487 doi:10.4319/lo.2002.47.3.0782

488 Hendy, E.J., Tomiak, P.J., Collins, M.J., Hellstrom, J., Tudhope, A.W., Lough, J.M.,
489 Penkman, K.E.H., 2012. Assessing amino acid racemization variability in coral intra-
490 crystalline protein for geochronological applications. *Geochim. Cosmochim. Acta* 86,
491 338–353. doi:10.1016/j.gca.2012.02.020

492 Hoegh-Guldberg, O., Muscatine, L., Goiran, C., Siggaard, D., Marion, G., 2004.
493 Nutrient-induced perturbations to delta C13 and delta N15 in symbiotic

494 dinoilagellates and their coral hosts. *Mar. Ecol. Prog. Ser.* 280, 105–114.
495 doi:10.3354/meps280105

496 Houlbrèque, F., Ferrier-Pagès, C., 2009. Heterotrophy in Tropical Scleractinian Corals.
497 *Biol. Rev.* 84, 1–17. doi:10.1111/j.1469-185X.2008.00058.x

498 Hughes, T.P., Baird, A.H., Bellwood, D.R., Card, M., Connolly, S.R., Folke, C.,
499 Grosberg, R., Hoegh-Guldberg, O., Jackson, J.B.C., Kleypas, J., Lough, J.M.,
500 Marshall, P., Nyström, M., Palumbi, S.R., Pandolfi, J.M., Rosen, B., Roughgarden, J.,
501 2003. Climate change, human impacts, and the resilience of coral reefs. *Science* 301,
502 929–933. doi:10.1126/science.1085046

503 Ingalls, A.E., Lee, C., Druffel, E., 2003. Preservation of organic matter in mound-
504 forming coral skeletons. *Geochim. Cosmochim. Acta* 67, 2827–2841.
505 doi:10.1016/S0016-7037(03)00079-6

506 Jupiter, S., Roff, G., Marion, G., Henderson, M., Schrameyer, V., McCulloch, M.,
507 Hoegh-Guldberg, O., 2008. Linkages between coral assemblages and coral proxies of
508 terrestrial exposure along a cross-shelf gradient on the southern Great Barrier Reef.
509 *Coral Reefs* 27, 887–903. doi:10.1007/s00338-008-0422-3

510 Kao, S.-J., Yang, J.-Y.T., Liu, K.-K., Dai, M., Chou, W.-C., Lin, H.-L., Ren, H., 2012.
511 Isotope constraints on particulate nitrogen source and dynamics in the upper water
512 column of the oligotrophic South China Sea. *Global Biogeochem Cycles* 26, GB2033.
513 doi:10.1029/2011GB004091

514 Karsh, K.L., Trull, T.W., Sigman, D.M., Thompson, P.A., Granger, J., 2014. The
515 contributions of nitrate uptake and efflux to isotope fractionation during algal nitrate
516 assimilation. *Geochim. Cosmochim. Acta* 132, 391–412.
517 doi:10.1016/j.gca.2013.09.030

518 Knapp, A.N., DiFiore, P.J., Deutsch, C., Sigman, D.M., Lipschultz, F., 2008. Nitrate
519 isotopic composition between Bermuda and Puerto Rico: Implications for N₂ fixation
520 in the Atlantic Ocean. *Global Biogeochem Cycles* 22, GB3014.
521 doi:10.1029/2007GB003107

522 Knapp, A.N., Sigman, D.M., Lipschultz, F., 2005. N isotopic composition of dissolved
523 organic nitrogen and nitrate at the Bermuda Atlantic Time-series Study site. *Global*
524 *Biogeochem Cycles* 19, GB1018. doi:10.1029/2004GB002320

525 Kopp, C., Pernice, M., Domart-Coulon, I., Djediat, C., Spangenberg, J.E., Alexander,
526 D.T.L., Hignette, M., Meziane, T., Meibom, A., 2013. Highly Dynamic Cellular-
527 Level Response of Symbiotic Coral to a Sudden Increase in Environmental Nitrogen.
528 *MBio* 4, e00052–13–e00052–13. doi:10.1128/mBio.00052-13

529 Logan, A., Yang, L., Tomascik, T., 1994. Linear skeletal extension rates in two species of

530 Diploria from high-latitude reefs in Bermuda. *Coral Reefs* 13, 225–230.
531 doi:10.1007/BF00303636

532 Lomas, M.W., Bates, N.R., Johnson, R.J., Knap, A.H., Steinberg, D.K., Carlson, C.A.,
533 2013. Two decades and counting: 24-years of sustained open ocean biogeochemical
534 measurements in the Sargasso Sea. *Deep Sea Res. Part II Top. Stud. Oceanogr.* 93,
535 16–32. doi:10.1016/j.dsr2.2013.01.008

536 Lorrain, A., Graham, B.S., Popp, B.N., Allain, V., Olson, R.J., Hunt, B.P.V., Potier, M.,
537 Fry, B., Galvan-Magana, F., Menkes, C.E.R., Kaehler, S., Menard, F., 2015.
538 Nitrogen isotopic baselines and implications for estimating foraging habitat and
539 trophic position of yellowfin tuna in the Indian and Pacific Oceans. *Deep Sea Res.*
540 *Part II Top. Stud. Oceanogr.* 113, 188–198. doi:10.1016/j.dsr2.2014.02.003

541 Marion, G.S., Dunbar, R.B., Mucciarone, D.A., Kremer, J.N., Lansing, J.S., Arthawiguna,
542 A., 2005. Coral skeletal delta N-15 reveals isotopic traces of an agricultural
543 revolution. *Mar. Pollut. Bull.* 50, 931–944. doi:10.1016/j.marpolbul.2005.04.001

544 Minagawa, M., Wada, E., 1984. Stepwise enrichment of ^{15}N along food chains: Further
545 evidence and the relation between $\delta^{15}\text{N}$ and animal age. *Geochim. Cosmochim. Acta*
546 48, 1135–1140. doi:10.1016/0016-7037(84)90204-7

547 Montoya, J.P., Carpenter, E.J., Capone, D.G., 2002. Nitrogen fixation and nitrogen
548 isotope abundances in zooplankton of the oligotrophic North Atlantic. *Limnol.*
549 *Oceanogr.* 47, 1617–1628. doi:10.4319/lo.2002.47.6.1617

550 Muscatine, L., Goiran, C., Land, L., Jaubert, J., Cuif, J.-P., Allemand, D., 2005. Stable
551 isotopes ($\delta^{13}\text{C}$ and $\delta^{15}\text{N}$) of organic matrix from coral skeleton. *Proc. Natl.*
552 *Acad. Sci. U.S.A.* 102, 1525–1530. doi:10.1073/pnas.0408921102

553 Needoba, J.A., Sigman, D.M., Harrison, P.J., 2004. The mechanism of isotope
554 fractionation during algal nitrate assimilation as illuminated by the N-15/N-14 of
555 intracellular nitrate. *J. Phycol.* 40, 517–522. doi:10.1111/j.1529-8817.2004.03172.x

556 Rafter, P.A., Sigman, D.M., 2016. Spatial distribution and temporal variation of nitrate
557 nitrogen and oxygen isotopes in the upper equatorial Pacific Ocean. *Limnol.*
558 *Oceanogr.* 61, 14–31. doi:10.1002/lno.10152

559 Rafter, P.A., Sigman, D.M., Charles, C.D., Kaiser, J., Haug, G.H., 2012. Subsurface
560 tropical Pacific nitrogen isotopic composition of nitrate: Biogeochemical signals and
561 their transport. *Global Biogeochem Cycles* 26, GB1003. doi:10.1029/2010GB003979

562 Ramos-Silva, P., Marin, F., Kaandorp, J., Marie, B., 2013. Biomineralization toolkit: the
563 importance of sample cleaning prior to the characterization of biomineral proteomes.
564 *Proc. Natl. Acad. Sci. U.S.A.* 110, E2144–6. doi:10.1073/pnas.1303657110

565 Ren, H., Sigman, D.M., Thunell, R.C., Prokopenko, M.G., 2012. Nitrogen isotopic

566 composition of planktonic foraminifera from the modern ocean and recent sediments.
567 *Limnol. Oceanogr.* 57, 1011–1024. doi:10.4319/lo.2012.57.4.1011

568 Reynaud, S., Martinez, P., Houlbreque, F., Billy, I., Allemand, D., Ferrier-Pagès, C.,
569 2009. Effect of light and feeding on the nitrogen isotopic composition of a
570 zooxanthellate coral: role of nitrogen recycling. *Mar. Ecol. Prog. Ser.* 392, 103–110.
571 doi:10.3354/meps08195

572 Sherwood, O.A., Guilderson, T.P., Batista, F.C., Schiff, J.T., McCarthy, M.D., 2014.
573 Increasing subtropical North Pacific Ocean nitrogen fixation since the Little Ice Age.
574 *Nature* 505, 78–81. doi:10.1038/nature12784

575 Sigman, D.M., Casciotti, K.L., Andreani, M., Barford, C., Galanter, M., Böhlke, J.K.,
576 2001. A bacterial method for the nitrogen isotopic analysis of nitrate in seawater and
577 freshwater. *Anal. Chem.* 73, 4145–4153. doi:10.1021/ac010088e

578 Smart, S.M., Fawcett, S.E., Thomalla, S.J., Weigand, M.A., Reason, C.J.C., Sigman,
579 D.M., 2015. Isotopic evidence for nitrification in the Antarctic winter mixed layer.
580 *Global Biogeochem Cycles* 29, 427–445. doi:10.1002/2014GB005013

581 Tambutte, S., Holcomb, M., Ferrier-Pagès, C., Reynaud, S., Tambutte, E., Zoccola, D.,
582 Allemand, D., 2011. Coral biomineralization: From the gene to the environment. *J.*
583 *Exp. Mar. Biol. Ecol.* 408, 58–78. doi:10.1016/j.jembe.2011.07.026

584 Tanaka, Y., Miyajima, T., Koike, I., Hayashibara, T., Ogawa, H., 2006. Translocation
585 and conservation of organic nitrogen within the coral-zooxanthella symbiotic system
586 of *Acropora pulchra*, as demonstrated by dual isotope-labeling techniques. *J. Exp.*
587 *Mar. Biol. Ecol.* 336, 110–119. doi:10.1016/j.jembe.2006.04.011

588 Wang, X.T., Prokopenko, M.G., Sigman, D.M., Adkins, J.F., Robinson, L.F., Ren, H.,
589 Oleynik, S., Williams, B., Haug, G.H., 2014. Isotopic composition of carbonate-
590 bound organic nitrogen in deep-sea scleractinian corals: A new window into past
591 biogeochemical change. *Earth Planet. Sci. Lett.* 400, 243–250.
592 doi:10.1016/j.epsl.2014.05.048

593 Wang, X.T., Sigman, D.M., Cohen, A.L., Sinclair, D.J., Sherrell, R.M., Weigand, M.A.,
594 Erler, D.V., Ren, H., 2015. Isotopic composition of skeleton-bound organic nitrogen
595 in reef-building symbiotic corals: A new method and proxy evaluation at Bermuda.
596 *Geochim. Cosmochim. Acta* 148, 179–190. doi:10.1016/j.gca.2014.09.017

597 Yamazaki, A., Watanabe, T., Tsunogai, U., 2011. Nitrogen isotopes of organic nitrogen
598 in reef coral skeletons as a proxy of tropical nutrient dynamics. *Geophys Res Lett* 38,
599 L19605. doi:10.1029/2011GL049053

600 Yoshikawa, C., Makabe, A., Shiozaki, T., Toyoda, S., Yoshida, O., Furuya, K., Yoshida,
601 N., 2015. Nitrogen isotope ratios of nitrate and N* anomalies in the subtropical South

604 **Figure Captions**

605

606 **Figure 1.** Locations and average coral skeletal $\delta^{15}\text{N}$ (CS- $\delta^{15}\text{N}$, ‰ vs. air) in each coral
607 core or set of cores used in this study.

608

609 **Figure 2.** Comparison of site-average coral skeletal $\delta^{15}\text{N}$ (CS- $\delta^{15}\text{N}$) with subsurface
610 nitrate $\delta^{15}\text{N}$. The annual mean surface nitrate concentrations in the adjacent
611 open ocean are below 0.5 μM for all the corals sites (filled circles) except for Kiritimati
612 Island (open circles). Thus, subsurface nitrate $\delta^{15}\text{N}$ is used as the x-axis parameter for all
613 corals sites except for Kiritimati Island. In the central equatorial Pacific, the surface
614 nitrate is not fully consumed; thus both nitrate and PON are available to Kiritimati corals
615 as their potential N sources. As it is unclear whether corals rely on nitrate assimilation or
616 feeding as their primary N sources at Kiritimati, both the $\delta^{15}\text{N}$ of instantaneous PON
617 (labeled with *) as calculated from the Rayleigh model (**Figure 3B**) and the average $\delta^{15}\text{N}$
618 of mixed layer nitrate measured at a set of stations adjacent to Kiritimati (155 °W, 0-1 °N,
619 labeled with **, **Figure 3B**) is used as the x-axis parameter (Rafter and Sigman, 2016).
620 The y-axis errors (1sd) are calculated from the CS- $\delta^{15}\text{N}$ data at each site while the x-axis

621 errors (1sd) are calculated from available nitrate $\delta^{15}\text{N}$ data (**Table 1**). With regard to the
622 latter, the actual uncertainty is likely greater due to spatial and temporal variation, and
623 additional N sources (e.g. coastal N inputs) and the effects of coastal N cycling have not
624 been addressed. These uncertainties are generally greatest for the corals from continental
625 margins.

626

627 **Figure 3.** (A) Bathymetry map of central equatorial Pacific and our coral site (Kiritimati
628 Island). White contours are climatological annual mean mixed layer nitrate
629 concentrations (World Ocean Atlas 2013). (B) Rayleigh model for nitrate consumption in
630 the central equatorial Pacific (Initial condition: $[\text{NO}_3^-] = 12.4 \mu\text{M}$; nitrate $\delta^{15}\text{N} = 7.2\text{‰}$;
631 isotope effect = 6.0‰ (Rafter and Sigman, 2016)). The blue, green and purple lines
632 correspond to the residual nitrate, instantaneous PON and integrated PON, respectively.
633 The vertical dashed line corresponds to the climatological annual mean mixed layer
634 nitrate concentration adjacent to the coral site. Open black circles denote nitrate $\delta^{15}\text{N}$ and
635 concentration measurements from 0 to 150 m at a set of stations close to Kiritimati (155
636 $^\circ\text{W}$, $0\text{-}1^\circ\text{N}$) (Rafter and Sigman, 2016).

637

638 **Figure 4.** Monthly variation in coral skeletal $\delta^{15}\text{N}$ and adjacent open ocean mixed layer

639 nitrate concentration over a one-year window from near Oman in the Arabian Sea. Nitrate
640 concentration data from open ocean waters adjacent to the coral site are from World
641 Ocean Atlas 2013. Shaded area indicates the southwest monsoon period (late June to
642 early October). Red dashed line indicates the subsurface nitrate $\delta^{15}\text{N}$ in the adjacent
643 Arabian Sea {Brandes:1998el}. The uncertainty of the coral chronology is estimated
644 to be 2 months. The CS- $\delta^{15}\text{N}$ change is small ($\sim 0.5\%$) and in the opposite sense expected
645 if the reef were considered to be bathed by nitrate-rich waters. For this and other reasons,
646 the Oman coral was grouped with the corals from open ocean settings of regionally
647 complete nitrate consumption. One possible explanation for the weak rise in CS- $\delta^{15}\text{N}$
648 during the summer monsoon period is that rapid feeding by the coral outpaced the
649 ammonium assimilation of the symbionts, leading to efflux of low $\delta^{15}\text{N}$ ammonium and a
650 slight rise in the $\delta^{15}\text{N}$ of the coral host/symbiont system (Wang et al., 2015). However,
651 lacking further information, other possibilities cannot be ruled out.

652

Table 1 Sample information and $\delta^{15}\text{N}$ data

Ocean Region	Coral Location	Coral core/colony #	Latitude	Longitude	Depth (m)	Coral species	Year of collection	Number of coral samples analyzed in each core	Sampling time-scale	Core-average skeletal $\delta^{15}\text{N}$ (‰, $\pm 1\sigma$)	Site-average skeletal $\delta^{15}\text{N}$ (‰, $\pm 1\sigma$)	$\delta^{15}\text{N}$ of oceanic N supply to the reefs (‰, $\pm 1\sigma$)	References for the $\delta^{15}\text{N}$ of oceanic N supply
North Atlantic	Bermuda ¹	1	32.46 N	64.83 W	10	<i>Diploria labyrinthiformis</i>	2005	10	annual, 1995-2005	3.7 \pm 0.5	4.1 \pm 0.50	2.5 \pm 0.2	Knapp et al., 2005
		2	32.46 N	64.83 W	10	<i>Diploria labyrinthiformis</i>	2005	10	annual, 1995-2005	3.9 \pm 0.4			
		3	32.46 N	64.83 W	10	<i>Diploria labyrinthiformis</i>	2005	10	annual, 1995-2005	3.5 \pm 0.5			
		4	32.40 N	64.79 W	4	<i>Diploria labyrinthiformis</i>	2005	10	annual, 1995-2005	4.4 \pm 0.5			
		5	32.40 N	64.79 W	4	<i>Diploria labyrinthiformis</i>	2005	10	annual, 1995-2005	4.5 \pm 0.2			
		6	32.40 N	64.79 W	4	<i>Diploria labyrinthiformis</i>	2005	10	annual, 1995-2005	4.7 \pm 0.5			
South Atlantic	Brazil margin ²	1	23.78 S	45.13 W	4-6	<i>Mussismilia hispida</i>	2013	2	multiyear	8.3 \pm 0.2	8.8 \pm 0.8	6.8 \pm 0.2	Frame 2011, Smart et al., 2015
		2	23.78 S	45.13 W	4-6	<i>Madracis decactis</i>	2013	2	multiyear	9.4 \pm 0.1			
Central Equatorial Pacific ³	Kiritimati Island	1	1.87 N	157.40 W	9	<i>Porites. sp</i>	1998	20	annual, 1977-1997	13.4 \pm 0.5	13.4 \pm 0.5	11.0 \pm 0.5/16.2 \pm 1.8	Rafter and Sigman, 2015
South Pacific	Northern Great Barrier Reef	1	12.38 S	143.74 E	3-5	<i>Porites. sp</i>	1990	30	semi-annual, 1975-1990	5.9 \pm 0.2	6.2 \pm 0.4	6.1 \pm 0.2	Yoshikawa et al., 2015
		2	13.33 S	143.96 E	3-5	<i>Porites. sp</i>	1990	32	semi-annual, 1974-1990	6.6 \pm 0.3			
North Pacific	New Caledonia Green Island	1	20.42 S	164.03 E	5	<i>Isopora palifera</i>	1995	2	multiyear	6.2 \pm 0.3	6.2 \pm 0.3	6.1 \pm 0.2	Yoshikawa et al., 2015
		1	22.65 N	121.47 E	6	<i>Porites. sp</i>	2013	18	seasonal, 2009-2013	4.2 \pm 0.6	4.2 \pm 0.6	3.9 \pm 1.0	Ren et al., unpublished data
South China Sea	Dongsha Atoll	1	20.76 N	116.79 E	1	<i>Porites. sp</i>	2013	18	seasonal, 2009-2013	5.7 \pm 0.5	5.9 \pm 0.5	5.5 \pm 0.3	Ren et al., unpublished data
		2	20.70 N	116.89 E	1	<i>Porites. sp</i>	2013	18	seasonal, 2009-2013	5.6 \pm 0.4			
		3	20.74 N	116.75 E	4	<i>Porites. sp</i>	2013	18	seasonal, 2009-2013	6.5 \pm 0.3			
Arabian Sea	Oman margin	1	17.50 N	55.7 E	3	<i>Porites. sp</i>	1996	12	seasonal, 1984-1985 & 1993-1995	10.1 \pm 0.2	10.1 \pm 0.20	9.0 \pm 1.0	Brandes et al., 1998

1. At Bermuda, 10 coral cores/colonies from 4 sites were analyzed for skeletal $\delta^{15}\text{N}$, but only the two offshore sites data are shown here because we seek to compare the skeletal $\delta^{15}\text{N}$ to the $\delta^{15}\text{N}$ of open ocean nitrate supplied to the reefs. Please refer to Wang et al. (2015) for further details.

2. At the Brazil margin, two species of corals adjacent to each other were analyzed for skeletal $\delta^{15}\text{N}$.

3. In the central equatorial Pacific, the surface nitrate is only partially consumed; thus both nitrate assimilation and feeding may contribute to the N sources of the Kiritimati coral. Here, the coral skeletal $\delta^{15}\text{N}$ is compared with both the mixed layer nitrate $\delta^{15}\text{N}$ (16.2 \pm 1.8‰) at a set of stations adjacent to Kiritimati (155 °W, 0-1 °N) and the

Figure 1

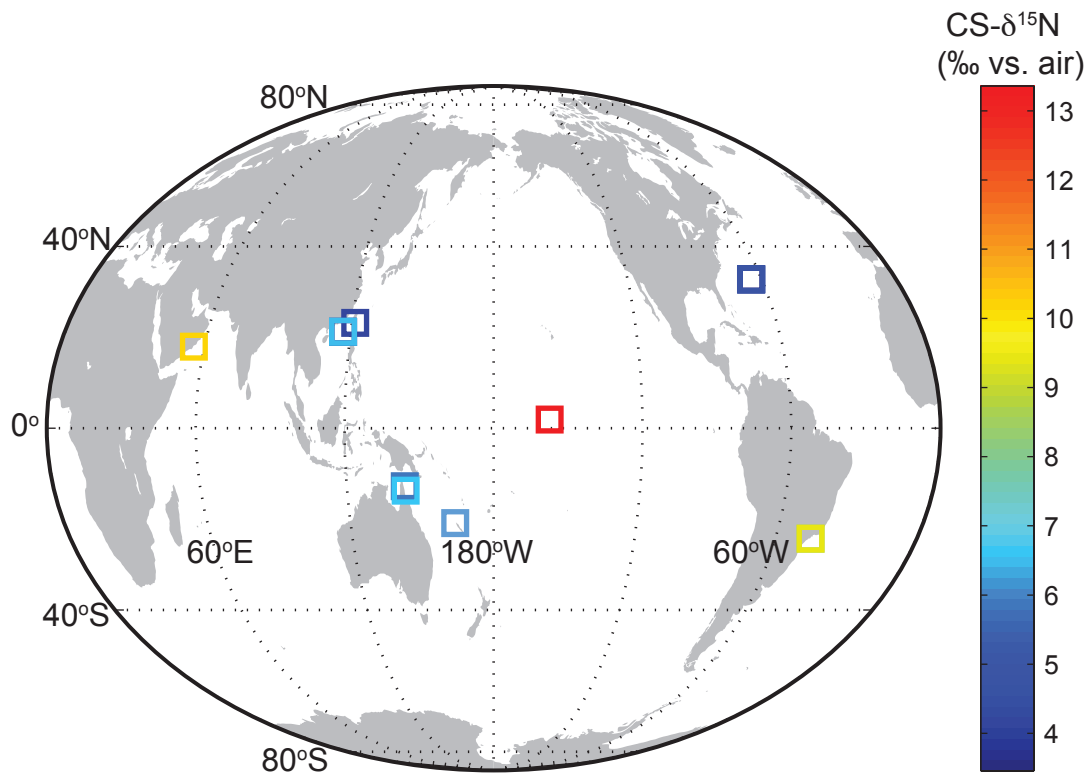


Figure 2

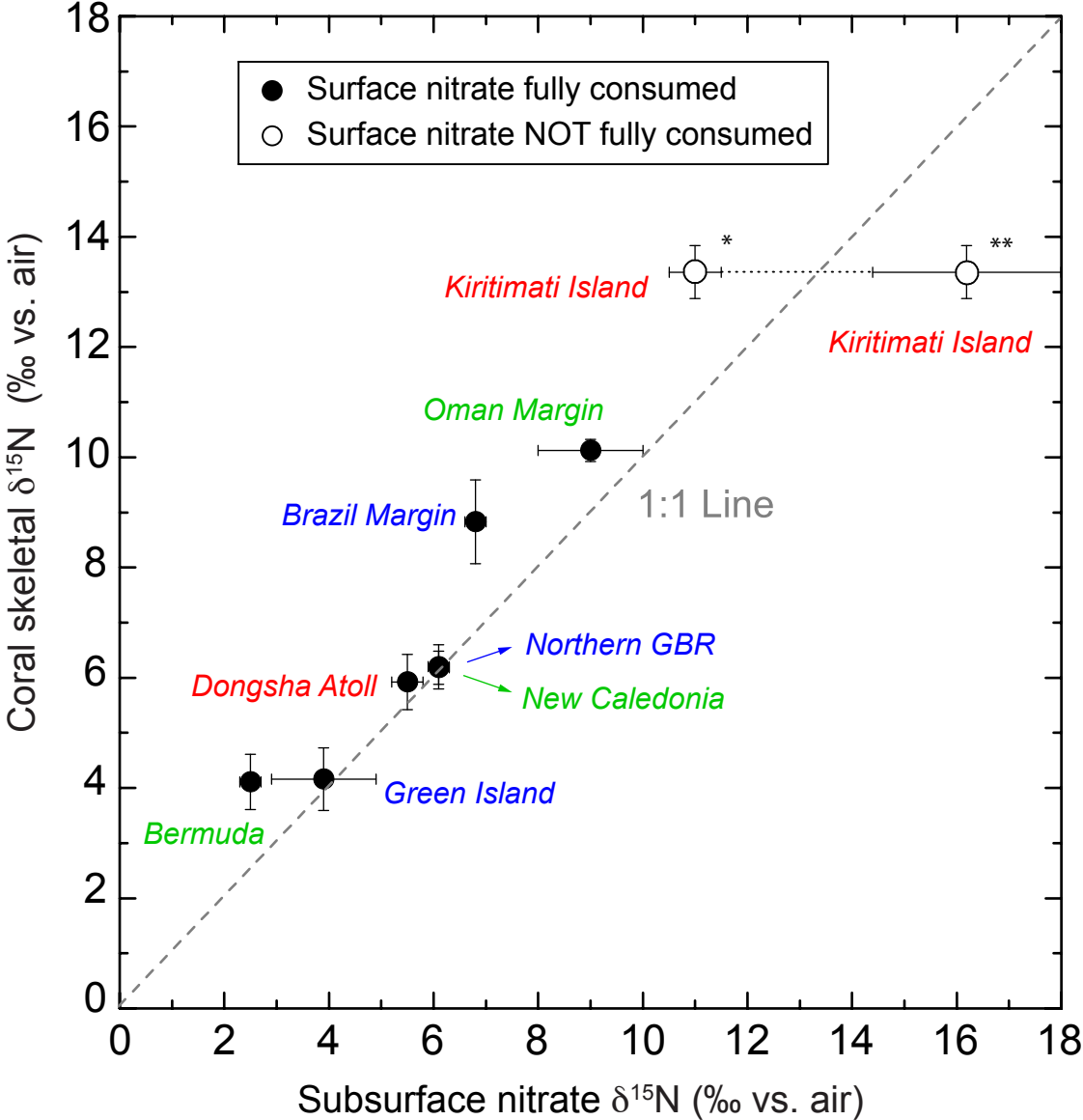


Figure 3

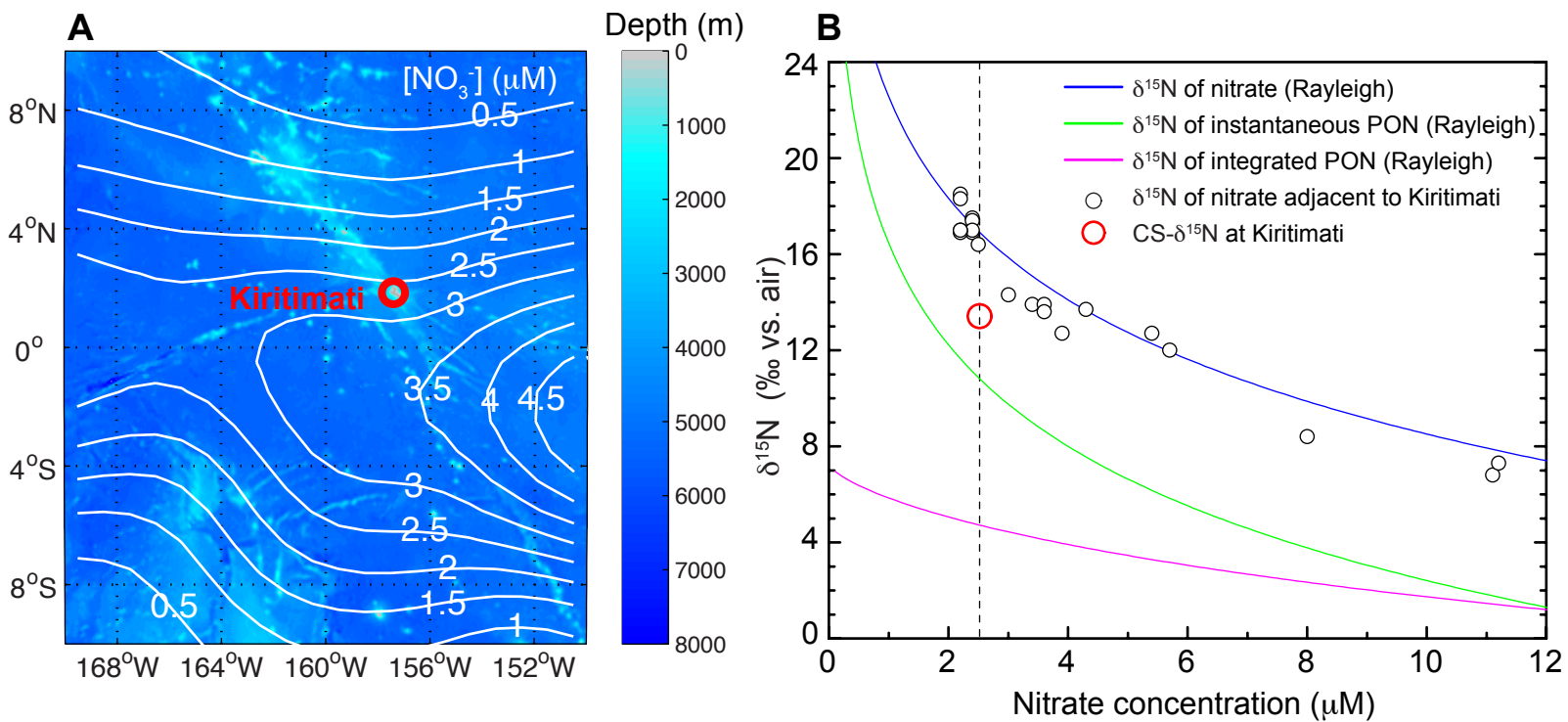


Figure 4

